Effect of Internal Bulk Phase on Surface Viscoelastic Properties by Scanning Probe Microscopy

Noriaki Satomi, Keiji Tanaka, Atsushi Takahara,† and Tisato Kajiyama*

Department of Applied Chemistry, Faculty of Engineering, Kyushu University, 6-10-1 Hakozaki, Higashi-ku, Fukuoka 812-8581, Japan

Received October 24, 2000; Revised Manuscript Received May 11, 2001

ABSTRACT: Scanning viscoelasticity microscopy (SVM) enables one to gain direct access to local viscoelastic properties on solid surfaces. In this study, it was demonstrated how deep the stimulus displacement by a cantilever tip propagated through a film. The glassy polymer/rubbery polymer bilayer prepared on silicon wafer was examined as a model system. Monodisperse polystyrene (PS) and polyisoprene (PI) were used as a glassy polymer for the outermost layer and a fully rubbery one for the underneath phase, respectively. The surface dynamic storage modulus, E', decreased with decreasing thickness of the upper PS layer due to the contribution from the soft underneath PI layer once the upper layer thickness fell short of 70 nm. On the contrary, surface E' was invariant for the bilayer with a thicker upper layer. These results indicate that the stimulus displacement imposed propagates to the depth of, at least, 70 nm along the surface normal at room temperature. The SVM measurement was also applied to monodisperse PS thin films with the number-average molecular weight of 140K spin-coated on silicon wafer with native oxide layer. In this case, while surface E' increased with a decrease in the thickness ranging from 80 nm down to 50 nm on account of the contribution from the hard substrate, it started to decrease for a thinner PS film. This result might imply that the PS surface and/or whole film started to soften up with decreasing thickness, in the case of a PS film thinner than 40 nm.

Introduction

A family of scanning probe microscope (SPM) has been extensively used for analyses of mechanical,[1−12] electrical,[13−15] and optical[16−18] properties at various material surfaces on the nanometer scale as well as conventional morphological observations.[19] Of the variety of these surface properties, surface rheology is crucial to design highly functionalized polymeric surfaces such as permselective membranes, biomaterials, lubricants, adhesives, etc. Hence, authors have explored surface molecular motion of various polymers based on deformation modulation technique of SPM, namely, scanning viscoelasticity microscopy (SVM).[4,20−25]

When the morphological observation is made under the contact mode, a tip indents into the sample surface, depending on how strong the normal force is applied onto the tip. That is, the sample surface is deformed by the tip. If either the sample stage or cantilever tip is sinusoidally modulated in this condition, the cyclic deformation is imposed to the sample surface. Since the amplitude of the cantilever response corresponding to the response force and the phase lag between the modulation displacement and response force signals are possible to be measured, dynamic viscoelastic functions at the polymer surface can be evaluated.[23] Another advantage of SVM is that dynamic viscoelastic functions at the surface can be two-dimensionally mapped by scanning the tip under the condition of the sample stage or tip modulation. Thus, SVM can identify different phases at multicomponent surfaces of polymer blends[20] and mixed monolayers[21] on the nanometer scale. However, surface viscoelastic properties of a system composed of a hard phase on a soft one have not been discussed yet. For instance, if the SVM measurement of a polystyrene (PS) slab floated on the water reservoir is carried out as an extreme case, how does the PS surface behave? Does it behave elastic- or viscous-like?

It seems reasonable to infer that surface viscoelastic properties are in the strong relation to the underneath aggregation state since the stimulation displacement might propagate deeply along the perpendicular direction to the surface. The question that should be addressed is, to what extent does such a displacement perpendicularly propagate through the film? The purpose of this study is to elucidate an influence of the internal structure on surface viscoelastic properties by SVM.

Experiment

Polymers used in this study were monodisperse PS synthesized by a living anionic polymerization and monodisperse polyisoprene (PI) purchased from Polymer Source, Inc. Table 1 collects the number-average molecular weight, M_n, the molecular weight distribution, M_w/M_n, where M_w denotes the weight-average molecular weight, and bulk glass transition temperature, T_g^b, of PS and PI. M_n and M_w/M_n were determined by gel permeation chromatography (GPC) with PS standards. T_g^b was evaluated by differential scanning calorimetry (DSC).

Two types of model films were prepared to examine the relation of internal rubbery phase to surface viscoelastic functions by SVM. Figure 1 illustrates the model systems employed: (a) mottled film and (b) bilayer film. The mottled film was prepared by mounting a PS thin film floated on the water upon a PI dewetted surface on silicon wafer with native oxide layer. The thickness of the upper PS layer was defined as the step height made by scratching the PS layer with a cantilever tip. The bilayer film was built up from a PS methyl ethyl ketone solution onto PI film supported on the clean silicon wafer by the spin-coating method. Since methyl ethyl ketone is a nonsolvent for PI, the PI layer is not seriously

* To whom correspondence should be addressed. Tel +81-92-642-3558; FAX +81-92-651-5606; E-mail kajiyama@cstf.kyushu-u.ac.jp.

† Current address: Institute for Fundamental Research of Organic Chemistry, Kyushu University.

10.1021/ma001831s CCC: $20.00
Published on Web 07/27/2001

Table 1. Characterizations of PS and PI Used in This Study

sample	M_n	M_w/M_n	T_g[b]/K
PS	140K	1.06	382
PI[a]	390K	1.06	210

[a] Purchased from Polymer Source, Inc.

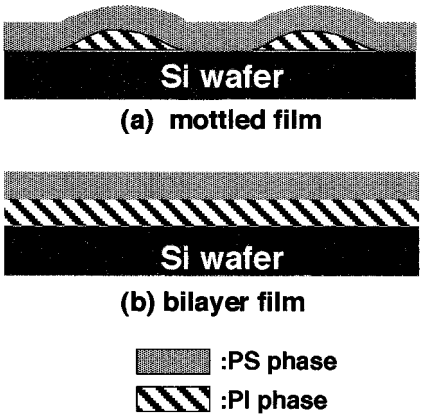

Figure 1. Schematic representation of the two model systems: (a) mottled film and (b) bilayer film.

damaged during the spin-coating process. The upper layer thickness of the bilayer film was evaluated by ellipsometric measurements. In both model systems, the thickness of the upper PS layer was controlled by changing the solution concentration.

Surface morphology of the model films was observed by an atomic force microscope (AFM). The AFM images were obtained by an SPA 300 with an SPI 3700 controller (Seiko Instruments Industry Co., Ltd.) at 293 K in air. Surface dynamic viscoelastic functions were evaluated by SVM measurement with the tip modulation mode. The normal force was fixed to be 10 nN. The modulation frequency and amplitude were 4 kHz and 1.0 nm, respectively. It was confirmed that the sample surface was not damaged during the SVM measurement. The cantilever tips used for AFM and SVM measurements were microfabricated from Si_3N_4, and their spring constants were determined to be 0.12 ± 0.03 N m^{-1} by Hutter and Bechhoefer's procedure.[26] Also, radii of curvature of cantilever tips were estimated to be 17.9 ± 3.8 nm on the basis of tip loci on colloidal gold nanoparticle with known size.[27] The details of the quantitative method for the surface modulus have been published elsewhere.[23]

Results and Discussion

Mottled Film. Before using the bilayer film, the mottled film is used as a model system. Since two regions underpinned with hard and soft phases are present at the surface, an effect of internal structure on surface viscoelastic functions can be easily seen in the SVM image, if any. In this section, after confirming whether the well-defined mottled structure is successfully prepared as shown in Figure 1a, the results are presented.

Since silicon and PI are in crystalline and rubbery states at room temperature, respectively, these phases can be distinguished on the basis of surface dynamic storage modulus, E'. Figure 2a shows the topographic image of the dewetted PI on the silicon wafer. The brighter part corresponds to the higher height region. The lateral size of the isolated domains is scattered, ranging from 100 nm to about 1 μm. On the other hand, the height of each dewetted domain is relatively monodispersed, such as 5−20 nm. Figure 2b shows the two-dimensional image of surface E' at the same field of view

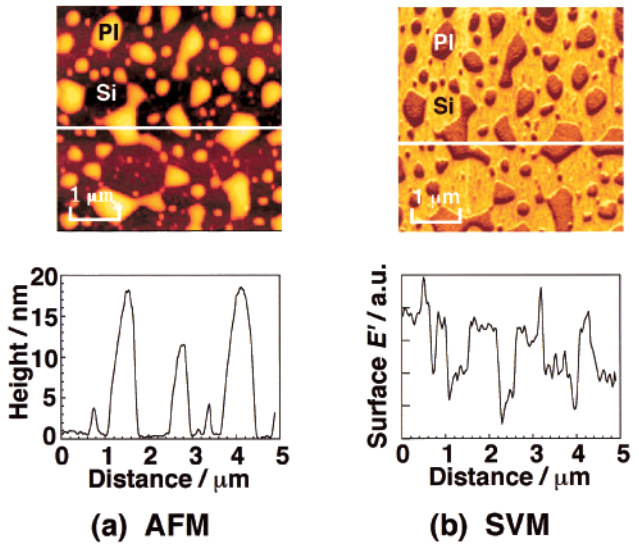

Figure 2. (a) Topographic (AFM) and (b) surface E' (SVM) images of dewetted PI on silicon wafer. Each line profile along the line in the corresponding image is displayed as well.

as the topographic image. Both images were simultaneously acquired at 293 K. In Figure 2b, the darker and brighter areas correspond to lower and higher E' regions, respectively. Since the darker regions of the SVM image correspond well to the droplet-like domains in the AFM image, it is clear that the domains and matrix in both images are assigned to the PI phases and the silicon substrate.

Parts a and b of Figure 3 display the surface morphology and their corresponding line profiles of the mottled films, which are defined as Figure 1a, with the 60 and 90 nm thick upper layers. The height and diameter of the protruded regions in Figure 3a seem to be in agreement with those of the PI phases in Figure 2a. Thus, it is conceivable that the upper PS layer is successfully mounted on the PI dewetted silicon wafer without serious corrugations. On the contrary, the apparent perimeter of the protruded regions in topographic images becomes larger when the thickness of the upper PS layer becomes thicker. Such a situation can be seen in the case of the 90 nm thick upper layer, as shown in Figure 3b. Besides, the smaller mottled regions, as seen in Figure 2a, disappear in Figure 3b. These results can be understood if the relative thick layer is successfully mounted on the PI dewetted surface. Figure 3c shows the SVM image of the mottled film with the thinner upper layer, 60 nm, and there exists a visible contrast in it. The contrast pattern in Figure 3c, which arose from the discrepancy of surface E', is similar to that in the topographical image of this specimen (Figure 3a). That is, the lower modulus regions in Figure 3c correspond well to the higher height ones in Figure 3a. Figure 3d shows the surface E' image of the mottled film with the upper PS layer of 90 nm thick. In contrast, this SVM image is completely homogeneous. Thus, it seems reasonable to conclude that surface viscoelastic functions based on our SVM are affected by the rubbery phase underneath the surface if such a soft region exists within the depth range shallower than 60 nm from the outermost surface.

Invoking that the response force can propagate as long as the stimulus deformation, the above-mentioned results suggest that the deformation might not propagate through the whole PS layer along the surface

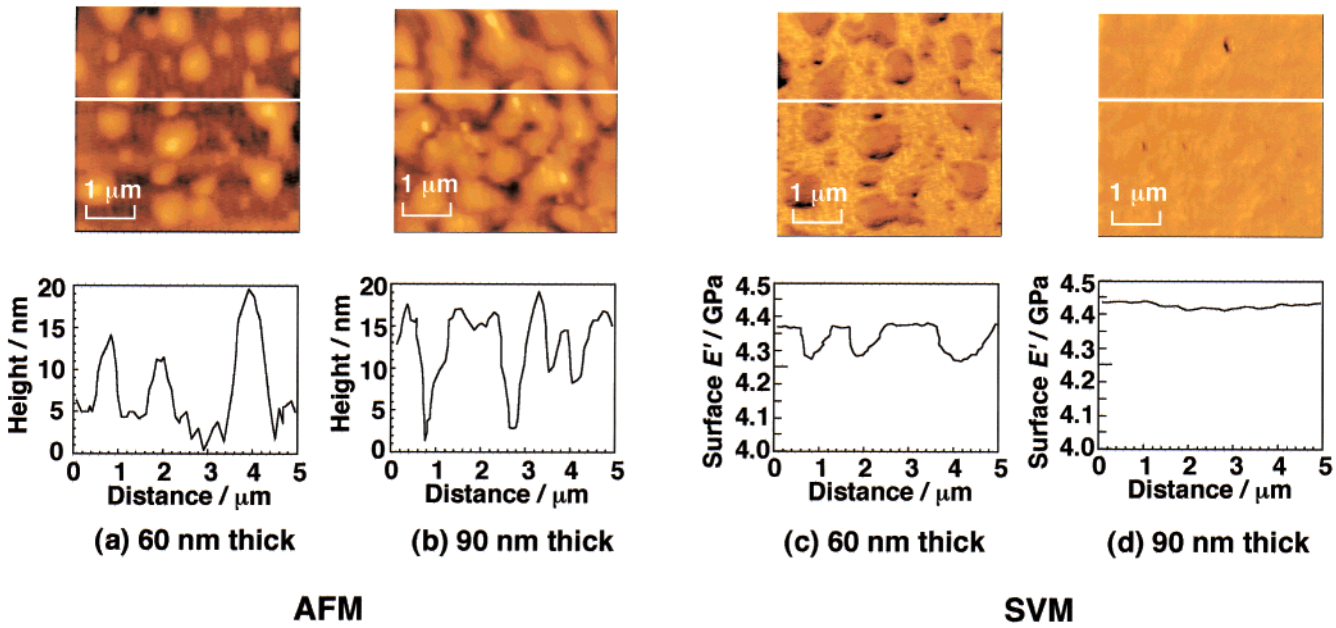

Figure 3. (a, b) AFM and (c, d) SVM images of the mottled films: (a, c) 60 nm thick upper layer; (b, d) 90 nm thick upper layer.

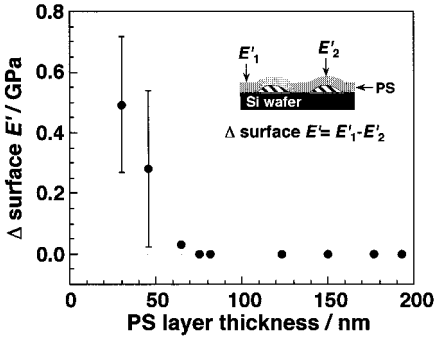

Figure 4. PS thickness dependence of Δ surface E' for the mottled film at 293 K.

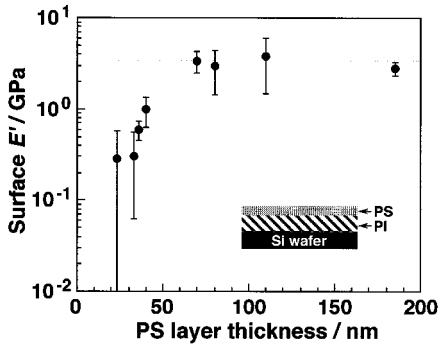

Figure 5. PS thickness dependence of surface E' for the (PS/PI) bilayer film at 293 K.

normal when the upper layer is thicker than 90 nm. However, this is not the case for the mottled film with the thinner upper PS layer such as 60 nm. In this case, the deformation could propagate wholly through the PS layer and then reach the underneath PI phase or silicon substrate, resulting in a discernible contrast in the surface E' image. To find the critical upper layer thickness in terms of the internal phase effect, SVM measurements for the mottled films with various upper layer thicknesses were carried out. Figure 4 shows Δ surface E' vs thickness of the upper PS layer. Here, Δ surface E' is defined as the discrepancy of surface E' between two apparent regions appeared in SVM image, namely, the darker and brighter regions. When the thickness of the upper PS layer fell short of 70 nm, Δ surface E' monotonically increased with decreasing upper layer thickness, as shown in Figure 4. Of course, this critical upper layer thickness depends on to what extent the normal force and/or the modulation amplitude are/is applied onto the sample surface. These results indicate that the special care should be taken to understand a result when the SVM measurement is applied to the multicomponent system in which a rubbery-like phase existed apart from the surface.

Bilayer Film. In the case of the mottled film, it might be possible that the deformation propagates toward not only the surface normal but also many other directions owing to the undulated surface morphology. In contrast, the bilayer film, which is our other model system, has the well-defined laminate structure. Thus, it seems likely that the deformation mainly propagates along the perpendicular direction to the surface, such the well-directed deformation makes a discussion facilitative. Figure 5 shows the surface E' variation with the upper glassy layer thickness for the bilayer film. When the upper layer thickness exceeded 70 nm, surface E' was invariant with respect to the upper layer thickness, and its magnitude was 3.2 ± 0.7 GPa. The corresponding surface E' for the PS thick film was previously found to be 4.5 ± 0.4 GPa.[22,23] Taking into account the deviation of tip radius and the measurement uncertainty of 10−20%, it is conceivable that surface E' of the (PS/PI) bilayer film is not influenced by the underneath PI layer if the upper PS layer is thicker than 70 nm. When the upper layer thickness for the (PS/PI) bilayer film became thinner, surface E' decreased with decreasing upper PS layer thickness. This trend is in good accordance with the result for the mottled film, as shown in Figure 4.

PS Thin Film. Finally, our SVM technique was applied to PS thin films directly spin-coated on the silicon wafer with native oxide layer. Figure 6 shows the film thickness dependence of surface E' for the PS films at 293 K. Surface E' started to increase at around 80 nm with decreasing film thickness because of the contribution from the hard silicon wafer which was connected in series to the PS film. However, in the case

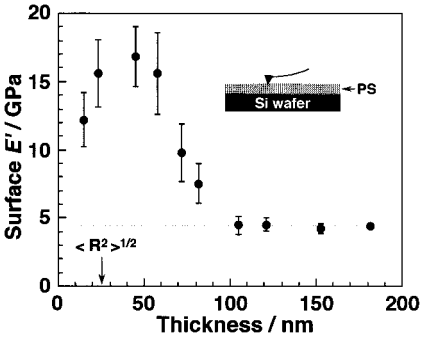

Figure 6. Thickness dependence of apparent surface E' for PS thin films spin-coated on silicon wafer with native oxide layer at 293 K. $\langle R^2 \rangle^{1/2}$ denotes the end-to-end distance of an unperturbed PS chain.

of a PS film thinner than 40 nm, which was a little larger than the end-to-end distance of an unperturbed PS chain, surface E' decreased with a decrease in the film thickness, as shown in Figure 6. That is, the maximum value was observed on the surface E'−film thickness relation. If viscoelastic properties of the PS film are independent of its thickness, surface E' obtained by SVM should be kept increasing with decreasing thickness, owing to increasing contribution of the hard silicon substrate. Hence, it can be envisaged that viscoelastic nature of a thinner PS film than 40 nm is different from that of the thick PS film. For the moment, it seems difficult to claim whether only the surface starts to soften up with decreasing film thickness when the thickness becomes thinner than approximately 40 nm or whether the whole film does. However, it is noteworthy that this trend is in good accordance with the film thickness dependence of physical properties such as T_g in PS thin films.[28]

Conclusions

An effect of internal bulk phase on surface E' by our SVM measurement was studied using two different model films. Surface E' was strongly dependent on the internal structure within 70 nm deep from the outermost surface under the current experimental condition. This result might be crucial information when SVM technique is applied to multicomponent systems such as polymer blends and copolymers. Also, SVM was applied to monodisperse PS thin films spin-coated on silicon wafer with native oxide layer. It was found that the surface and/or whole part of the film started to soften up as the film became thinner than 40 nm.

Acknowledgment. This was in part supported by Grant-in-Aids for COE Research (#08CE2005) and for Scientific Research (A) (#13355034) from the Ministry of Education, Science, Sports, and Culture, and by Research Fellowships of the Japan Society for the Promotion of Science for Young Scientists.

References and Notes

(1) Maivald, P.; Butt, H. J.; Gould, S. A. C.; Prater, C. B.; Drake, B.; Gurlev, J. A.; Elings, V. B.; Hansma, P. K. *Nanotechnology* **1991**, *2*, 103.
(2) Radmacher, M.; Tillmann, R. W.; Gaub, E. *Biophys. J.* **1993**, *64*, 735.
(3) Overney, R. M.; Meyer, E.; Frommer, J.; Güntherodt, H.-J.; Fujihira, M.; Takano, H.; Gotoh, Y. *Langmuir* **1994**, *10*, 1281.
(4) Kajiyama, T.; Tanaka, K.; Ohki, I.; Ge, S.-R.; Yoon, J.-S.; Takahara, A. *Macromolecules* **1994**, *27*, 7932.
(5) Friedenberg, M. C.; Mate, C. M. *Langmuir* **1996**, *12*, 6138.
(6) Burnham, N. A.; Kulik, A. J.; Gremaud, G.; Gallo, P.-J.; Oulevey, F. *J. Vac. Sci. Technol. B* **1996**, *14*, 794.
(7) Vanlandingham, M. R.; McKnight, S. H.; Palmese, G. R.; Elings, J. R.; Huang, X.; Bogetti, T. A.; Eduljee, R. F.; Gillespie, J. W. *J. Adhes.* **1997**, *64*, 31.
(8) Domke, J.; Radmacher, M. *Langmuir* **1998**, *14*, 3320.
(9) Hammerschmidt, J. A.; Gladfelter, W. L.; Haugstad, G. *Macromolecules* **1999**, *32*, 3360.
(10) Oulevey, F.; Burnham, N. A.; Gremaud, G.; Kulik, A. J.; Pollock, H. M.; Hammiche, A.; Reading, M.; Song, M.; Hourston, D. J. *Polymer* **2000**, *41*, 3087.
(11) Tsukruk, V. V.; Huang, Z. *Polymer* **2000**, *41*, 5541.
(12) Tsui, O. K. C.; Wang, X. P.; Ho, J. Y. L.; Ng, T. K.; Xiao, X. *Macromolecules* **2000**, *33*, 4198.
(13) Yokoyama, H.; Inoue, T. *Thin Solid Films* **1994**, *242*, 33.
(14) Inoue, T.; Itoh, J.; Yokoyama, H. *Nanotechnology* **1997**, *8*, A19.
(15) Kajiyama, T.; Khuwattanasil, N.; Takahara, A. *J. Vac. Sci. Technol. B* **1998**, *16*, 121.
(16) Betzig, E.; Trautman, J. K. *Science* **1992**, *257*, 189.
(17) Williamson, R. L.; Miles, M. J. *J. Vac. Sci. Technol. B* **1996**, *B14*, 809.
(18) DeAro, J. A.; Weston, K. D.; Buratto, S. K.; Lemmer, U. *Chem. Phys. Lett.* **1997**, *277*, 532.
(19) Ratner, B. D., Tsukruk, V. V., Eds. *Scanning Probe Microscopy of Polymer*; ACS Symp. Ser.; American Chemical Society: Washington, DC, 1998.
(20) Tanaka, K.; Yoon, J. S.; Takahara, A.; Kajiyama, T. *Macromolecules* **1995**, *28*, 934.
(21) Ge, S.-R.; Takahara, A.; Kajiyama, T. *Langmuir* **1995**, *11*, 1, 1341.
(22) Tanaka, K.; Taura, A.; Ge, S.-R.; Yoon, J.-S.; Takahara, A.; Kajiyama, T. *Macromolecules* **1996**, *29*, 3040.
(23) Kajiyama, T.; Tanaka, K.; Takahara, A. *Macromolecules* **1997**, *30*, 280.
(24) Tanaka, K.; Takahara, A.; Kajiyama, T. *Macromolecules* **1998**, *31*, 863.
(25) Satomi, N.; Takahara, A.; Kajiyama, T. *Macromolecules* **1999**, *32*, 4474.
(26) Hutter, J. L.; Bechhoefer, J. *Rev. Sci. Instrum.* **1993**, *64*, 1868.
(27) Vesenka, J.; Manne, S.; Giberson, R.; Marsh, T.; Henderson, E. *Biophys. J.* **1993**, *65*, 992.
(28) Forrest, J. A.; Jones, R. A. L. In *Polymer Surfaces, Interfaces and Thin Films*; Karim, A., Kumar, S., Eds.; World Scientific: Singapore, 2000; p 251.

MA001831S